Ferroelastic domain motion by pulsed electric field in (111)/(11$\bar{1}$) rhombohedral epitaxial $Pb(Zr_{0.65}Ti_{0.35})O_3$ thin films: Fast switching and relaxation

Yoshitaka Ehara,[1] Takao Shimizu,[2,3,*] Shintaro Yasui,[4] Takahiro Oikawa,[1] Takahisa Shiraishi,[1,5] Hiroki Tanaka,[1] Noriyuki Kanenko,[1] Ronald Maran,[6] Tomoaki Yamada,[7,8] Yasuhiko Imai,[9] Osami Sakata,[10] Nagarajan Valanoor,[6] and Hiroshi Funakubo[1,2,3,†]

[1]*Department of Innovative and Engineered Material, Tokyo Institute of Technology, Yokohama 226–8503, Japan*
[2]*Materials Research Center for Element Strategy, Tokyo Institute of Technology, Yokohama, 226–8503, Japan*
[3]*School of Materials and Chemical Technology, Tokyo Institute of Technology, Yokohama 226–8502, Japan*
[4]*Laboratory for Materials and Structures, Tokyo Institute of Technology, Yokohama 226–8503, Japan*
[5]*Institute for Materials Research, Tohoku University, 2-1-1 Katahira, Aoba-ku, Sendai 980–8577, Japan*
[6]*School of Materials Science and Engineering, University of New South Wales, NSW 2052 Sydney Australia*
[7]*Department of Energy Engineering, Nagoya University, Nagoya 464–8603, Japan*
[8]*PRESTO, Japan Science and Technology Agency, Kawaguchi 332–0012, Japan*
[9]*Japan Synchrotron Radiation Research Institute (JASRI), 1-1-1 Kouto, Sayo, Hyogo 679–5198, Japan*
[10]*Synchrotron X-ray Group and Synchrotron X-ray Station at SPring-8, National Institute for Materials Science (NIMS), 1-1-1 Kouto, Sayo, Hyogo, 679–5148, Japan*

(Received 1 July 2019; published 30 September 2019)

Reversible electric-field induced domain switching in ferroelectric thin films gives rise to a large electromechanical coupling. Despite extensive *in situ* studies confirming a dominant contribution from domain switching, the speed of the domain wall motion had not been discussed enough. In this study, we performed time-resolved measurement of lattice elongation and non-180° domain switching for an epitaxial rhombohedral (111)/(11$\bar{1}$)-oriented ($Pb(Zr_{0.65}Ti_{0.35})O_3$ film under nanosecond electric field pulses by means of synchrotron x-ray diffraction. Both lattice elongation and non-180° domain switching due to a 200-ns electric pulse were directly observed from the shift of the 222 diffraction position toward a lower angle and the change in the integrated intensity ratio of 222 to 22$\bar{2}$ peaks, respectively. The non-180° domain switching also results in an increase of the switchable polarization. Following the removal of the electric field, it is seen that the non-180° domain back switching from 222 to 22$\bar{2}$ is sluggish compared to the relaxation of the field-induced lattice strain. This is different from the (100)/(001)-oriented tetragonal epitaxial Pb(Zr, Ti)O_3 films, in which no obvious delay was detected. These results show the importance of the direct time-resolved response observation of the crystal structure change with the application of a high-speed electric pulse field to understand the frequency dispersion of the ferroelectric and piezoelectric responses of Pb(Zr, Ti)O_3 films.

DOI: 10.1103/PhysRevB.100.104116

I. INTRODUCTION

Thin films of ferroelectric materials have been applied to many electronic devices, including sensors and actuators and microelectromechanical systems (MEMS) [1]. Due to their outstanding dielectric and piezoelectric properties, $Pb(Zr_{1-x}Ti_x)O_3$ (PZT) films have been the most extensively investigated, especially for actuator applications.

It has been recognized that the macroscopic strain induced by an electric field in ferroelectric materials mainly consists of two different contributions: (i) an intrinsic effect including the change in the lattice spacing by application of the electric field and (ii) extrinsic effects such as ferroelastic motion, for instance, non-180° domain switching in a ferroelectric material. Among these two contributions, non-180° domain switching in PZT films, such as 90° domains in the tetragonal phase and 71° and 109° domains in the rhombohedral phase, have been demonstrated to contribute largely to the piezoelectric response [2,3]. For example, non-180° domain switching is reported to be responsible for more than 50% of the piezoelectric response [2]. It has been pointed out that non-180° domain switching responses generally decrease with increasing measurement frequency due to the pinning of non-180° domain wall motion [4–6]. Crystal structure change under an applied electric field has been investigated using *in situ* x-ray diffraction (XRD) measurements in both PZT ceramics [4,7–9] and films [10–14]. Lattice strain and non-180° domain switching under an applied electric field have been discussed based on *in situ* observation data in the case of PZT ceramics, for the rhombohedral [7,9] as well as the tetragonal phase [8]. The largest piezoresponse is found in compositions near the morphotropic phase boundary (MPB), which is the region that separates both the tetragonal and rhombohedral structures in the PZT phase diagram.

*Author to whom correspondence should be addressed: shimizu.t.aa@m.titech.ac.jp
†funakubo.h.aa@m.titech.ac.jp

Despite many studies focused on *in situ* observation under an electric field, time dynamics of non-180° domain wall motion is not sufficiently understood from a crystallographic viewpoint. On one hand, the piezoelectric and dielectric responses take advantage of such domain wall motions, on the other hand, the domain wall motions are difficult to apply for high-speed devices because of their remarkable frequency dispersion. The frequency dependence of ferroelastic 90° domain switching has been reported for ceramics in the low-frequency range from 0.06 to 3 Hz; the contribution of 90° domain switching decreased from 75 to 64% as the frequency increased [4]. In the case of films, tetragonal PZT has been studied by direct measurement of the lattice strain [11–13] and non-180° domain switching [10,14]. Recent reports of tetragonal ferroelectric films have shown that the non-180° domain can be switched on the order of tens of nanoseconds [15–17].

The $(111)/(11\bar{1})$ domain switching has been reported to largely contribute piezoelectric responses in rhombohedral phases [18,19]. The remarkable frequency dispersion has been reported for the dielectric constant of rhombohedral PZT ceramics compared to the tetragonal ones, implying that the domain switching does not follow high-frequency signals [20,21]. PZT films with MPB composition often include both tetragonal and rhombohedral phases, so that the frequency-dependent domain switching in the rhombohedral structure is important even for the MPB composition. Thus, it is crucial for high-speed piezo-MEMS applications to observe directly fast $(111)/(11\bar{1})$ domain switching in the rhombohedral phase by applying an electric field.

In this study, we directly investigated the time responses of the crystal lattice and ferroelastic domain to an applied electric field in an epitaxial PZT film with rhombohedral symmetry by means of *in situ* synchrotron XRD measurement. We found a large increase in the fraction of the (111)-oriented domain from the $(11\bar{1})$-oriented domain that is induced by an electric field as well as elongation of the lattice length. The intrinsic lattice elongation immediately responded to both the application and the removal of the electric field. The volume fraction of the (111)-oriented domain increased by the application of the electric field within the rise time without delay, while it returned to an original value with a marked delay following the removal of the electric field. The relaxation time of the domain back switching based on the single relaxation model agrees with the time for the electric polarization, whereas it is much larger than the falling time for electric pulses. This delay in the switching back of the ferroelastic domain shows a clear contrast to the fast relaxation of the ferroelastic domain in the tetragonal PZT. The difference between rhombohedral and tetragonal phases underpins the varying frequency dispersion in both the dielectric and piezoelectric responses in PZT thin films, and perhaps PZT bulk ceramics.

II. EXPERIMENTAL

The sample was a $(111)/(11\bar{1})$-oriented epitaxial rhombohedral $Pb(Zr_{0.65}Ti_{0.35})O_3$ (PZT65/35) film with 200-nm thickness grown on a $(111)_c SrRuO_3//(111)KTaO_3$ substrate by pulsed-metal organic chemical vapor deposition (MOCVD). Details of the sample preparation are described elsewhere [22]. The sheet resistance and thickness of the bottom $SrRuO_3$ electrode is about 60 Ω and 50 nm, respectively. The electrical characterization was performed for the tetragonal $Pb(Zr_{0.4}Ti_{0.6})O_3$ films prepared by MOCVD, whose time-resolved measurements were already reported [17].

The orientation of the deposited films was analyzed by XRD using a four-axis diffractometer (PANalytical X'Pert MRD). XRD reciprocal space mappings, XRD-RSMs, were measured to estimate the volume fraction of the (111) orientation (V_{111}). Polarization-electric field (***P*-*E***) loops were measured using a ferroelectric tester (Toyo Corp. FCE-1). For the electrical characterizations, 100-μm-diameter Pt top electrodes were fabricated by electron-beam evaporation.

In situ observation of the lattice strain and non-180° domain switching under an applied electric field was carried out at the BL13XU in SPring-8. In order to acquire the electric-field-induced modification in diffraction data, an incident beam with the photon energy of 12.4 keV ($\lambda = 1$ Å) was focused on an area $2 \times 3\ \mu m^2$ in width and height using a two-dimensional focusing refractive lens and positioned on the Pt top electrode by monitoring the fluorescent x-ray. We applied the pulse voltages of a magnitude of 20 V and monitored the change in $22\bar{2}$ and 222 peaks under the voltage applications. The repetitive electric pulses were applied with repetition rate of 1.25 MHz (interval of pulses is 800 ns). The 200-ns square pulse electric field was applied using a pulse generator (Agilent, 8114A) and FCE-HS3 (Toyo, 6321). Details of the setup for the time-resolved synchrotron x-ray diffraction measurement have already been described elsewhere [23].

III. RESULTS AND DISCUSSIONS

XRD-RSM around 222 $KTaO_3$ diffraction for PZT65/35 films is shown in Fig. 1(a). There are 222 PZT, $22\bar{2}$ PZT, 222_c $SrRuO_3$, and 222 $KTaO_3$ peaks in Fig. 1(a), suggesting the growth of $(111)/(11\bar{1})$-oriented films. Both of the 222 and $22\bar{2}$ peaks have the maxima at the $q_x = 0$, indicating that the (111) and $(11\bar{1})$ domains do not tilt with respect to the surface of the substrate. This result agrees with the previous study [24]. In-plane alignment of these films, i.e., epitaxial film growth, was ascertained by x-ray pole figure measurement, suggesting the growth of epitaxial $(111)/(11\bar{1})$-oriented rhombohedral PZT65/35 [see Figs. 1(b) and 1(c)]. The volume fraction of the 111 orientations (V_{111}) in the PZT film as the virgin state was obtained from the integrated intensity ratio 222 and $22\bar{2}$. V_{111} is given by the following equation:

$$\boldsymbol{V}_{111} = \frac{\frac{\boldsymbol{I}_{222}}{\boldsymbol{I}'_{222}}}{\frac{\boldsymbol{I}_{222}}{\boldsymbol{I}'_{222}} + 3\frac{\boldsymbol{I}_{22\bar{2}}}{\boldsymbol{I}'_{22\bar{2}}}}, \tag{1}$$

where I_{hkl} and I'_{hkl} represent the integrated intensity of observed *hkl* reflection peak and the reference integrated intensity of *hkl* reflection in random orientation, respectively [18,25]. I_{hkl} is estimated by the peak fitting with two Lorentz functions, while I'_{hkl} is calculated from the reported crystal structure [26]. $V_{111} = 0.1$ was estimated from the integrated intensities shown in Fig. 1(a) taking into account the multiplicity factors of one and three for 222 and $22\bar{2}$, respectively. The low V_{111} value of the as-deposited films can be explained by the thermal strain (ε_t) at the Curie temperature

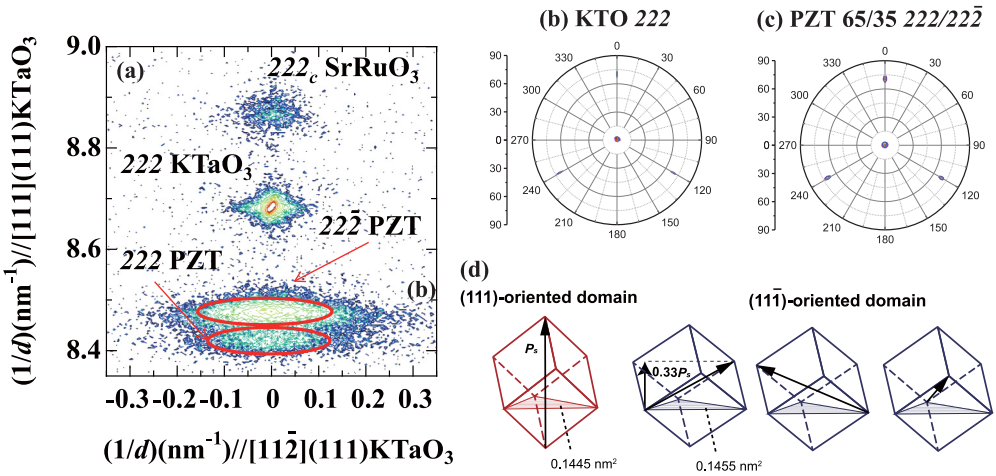

FIG. 1. (a) High-resolution XRD reciprocal space mapping around 222 $KTaO_3$, XRD pole figures measured for (b) KTO 222 reflections and (c) PZT65/35 222/$22\bar{2}$ reflections, (d) schematic representation of the domain structure in a film with (11$\bar{1}$) and (111) domains. The hatched regions in panel (b) represent the (111) and (11$\bar{1}$) planes contacting with the substrate.

accumulated during the cooling process after the film deposition; the volume fraction of (111)-orientation (V_{111}) in (11$\bar{1}$)/(111) mixed orientations linearly changed with ε_t at the Curie temperature [27]. Figure 1(d) shows the schematics of expected domains in the rhombohedral structure. The direction of the spontaneous polarization of the (111)-orientation is aligned with the surface normal direction, while the projection of the spontaneous polarization of (11$\bar{1}$)-orientation is 33%, where the spontaneous polarization is tilted by 71° from the surface normal direction, as illustrated in Fig. 1(d) [26].

Figure 2(a) shows room-temperature ***P*-*E*** hysteresis loops measured for the rhombohedral PZT 65/35 at 1 kHz. The $\boldsymbol{P}_{\max}$ value at $\boldsymbol{E}_{\max}$ of 1 MV/cm was 66 μC/cm^2 and the $\boldsymbol{P}_r$ value after removal was 33 μC/cm^2. Both P_r of 33 μC/cm^2 and $\boldsymbol{P}_{\max}$ of 66 μC/cm^2 observed in this study is too large, by taking into account the observed V_{111} and spontaneous polarization. The saturation curves for both $\boldsymbol{P}_r$ and $\boldsymbol{P}_{\max}$ are also displayed in Fig. 2(b). The large $\boldsymbol{P}_r$ indicates the irreversible change in the domain fraction by the poling process as observed in a previous study [4]. Furthermore, the large difference between $\boldsymbol{P}_r$ and $\boldsymbol{P}_{\max}$ and their nonlinear relationship indicated reversible non-180° domain switching, as such behavior cannot be explained by the simple increase of polarization strength by the application of the electric field, which typically shows close to a linear behavior.

In order to reveal the difference in the response of the non-180° domain switching for the tetragonal and rhombohedral PZT, we compared the ***P*-*E*** characteristics. Figures 2(c) and 2(d) show the ***P*-*E*** hysteresis loops measured with the unipolar electric field at various frequencies from 1 to 100 kHz for (001)/(100)-oriented epitaxial tetragonal PZT40/60 and (111)/(11$\bar{1}$)-oriented epitaxial rhombohedral PZT65/35, respectively. The tetragonal PZT40/60 shows the linear dielectric response with almost constant $\boldsymbol{P}_{\max}$, having small frequency dispersion, although the 90° domain switching was confirmed by the previous *in situ* XRD measurement. On the contrary, the rhombohedral PZT showed a nonlinear dielectric response with hysteresis. In addition, the $\boldsymbol{P}_{\max}$ value decreased from 35 to 20 μC/cm^2 with an increase in the frequency from 1 to 100 kHz. These results imply the different frequency dispersion in non-180° domain wall motions between the tetragonal and rhombohedral PZT. Figure 2(e) summarizes the frequency dependences of maximum polarization for both tetragonal PZT40/60 and rhombohedral PZT65/35. The polarization of tetragonal films shows small change from 4.8 μC/cm^2 at 1 kHz to 4.4 μC/cm^2 at 100 kHz with increasing measurement frequency. On the other hand, the rhombohedral films show a drastic decrease from 35 μC/cm^2 at 1 kHz to 25 μC/cm^2 at 100 kHz. It is noted the domain wall motion in the PZT shows logarithmic decrease with respect to the frequency. The observed monotonic decrease of the dielectric responses does not contradict the model [28,29].

Figure 3(a) shows the XRD pattern near 222 and $22\bar{2}$ diffraction peaks as a function of measurement time during repeat application of pulsed voltage with 20 V (1 MV/cm) amplitudes for rhombohedral PZT65/35 film after application of 1.2 MV/cm (after measuring *P*-*E* loops shown in Fig. 2(a) corresponding to post-poling treatment). The wave form for the pulse electric field is displayed at the upper right of Fig. 3(a). At 0 ns, just before the electric field and after the poling, V_{111} was estimated to be 0.33, greater than the virgin state shown in Fig. 1(a), $V_{111} = 0.1$, due to the irreversible change in the domain fraction by the poling process as explained above.

As shown in Fig. 3(a), the positions and intensities of the diffraction were clearly changed by the application of an electric field due to the change of the lattice parameter and non-180° domain switching, respectively. The θ-2θ diffractograms at several time periods (scan *I*: 20 ns, scan *II*: 100 ns, scan *III*: 150 ns, scan IV: 300 ns, scan *V*: 700 ns) extracted from Fig. 3(a) are plotted in Fig. 3(b). Here the time standard was given by the trigger signal from the pulse generator. During the period of the applied electric field (scans *II* and *III*), the peak position of 222 shifted to a lower angle, while no significant shift for $22\bar{2}$ was seen. This shows the elongation of the (111)-oriented domain, the polar-axis-oriented domain of the rhombohedral phase, and the lack of elongation for the (11$\bar{1}$)-oriented domain, even though it has a nonzero surface

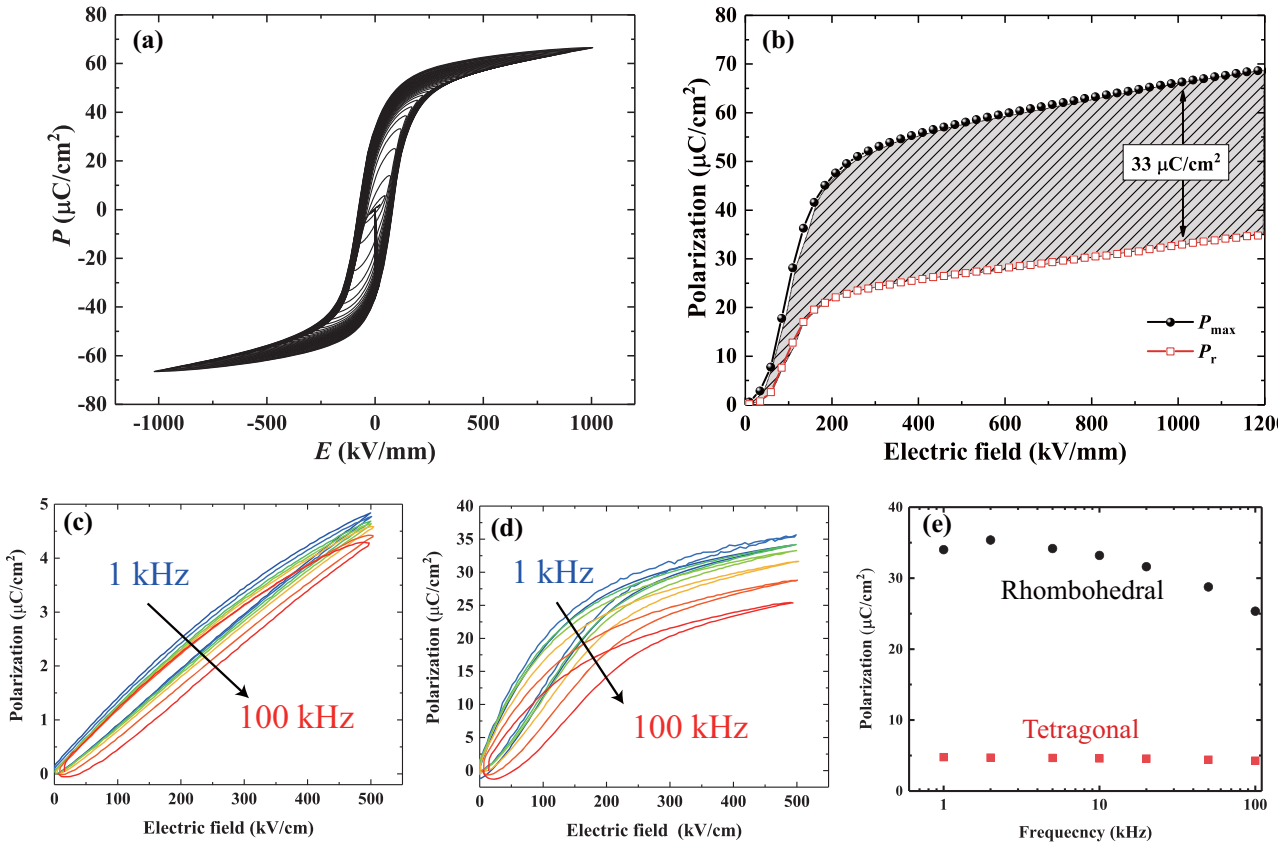

FIG. 2. (a) Room temperature ***P–E*** hysteresis loops measured at 1 kHz, and (b) change of remanent polarization (P_r) and maximum polarization ($P_{max.}$) as a function of applied maximum electric field ($E_{max.}$) obtained from (a). The unipolar ***P–E*** curves measured for the (c) (001)/(100)-oriented epitaxial tetragonal PZT40/60 and (d) (111)/(11$\bar{1}$)-oriented epitaxial rhombohedral PZT 35/65 at a various frequency from 1 kHz to 100 kHz. (e) Frequency dependence of the maximum polarization for rhombohedral and tetragonal PZT.

normal component of polarization, as schematically shown in Fig. 1(d). On the other hand, the intensity ratio of 222 and 22$\bar{2}$ peaks increased and decreased, respectively, suggesting the non-180° domain switching from (11$\bar{1}$)- to (111)-oriented domains. In addition, the 222 reflection peak seemed to be broaden compared to the initial state (indicated by scan *I*).

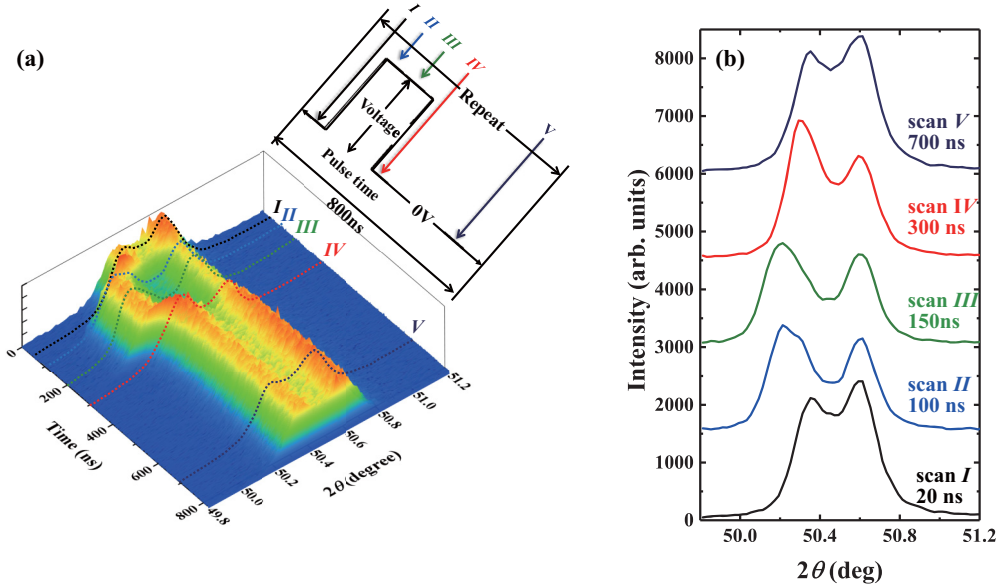

FIG. 3. (a) Three-dimensional intensity contour map of *in situ* XRD study as a function of 2θ and time. The wave form of the application of the square pulse voltage is depicted. The more than 10^{10} electric pulses with 200 ns in width were applied repeatedly by interval of 800 ns. (b) θ-2θ profiles at several time periods (scan *I*:20 ns, scan *II*:100 ns, scan *III*:150 ns, scan IV:300 ns, scan *V*:700 ns).

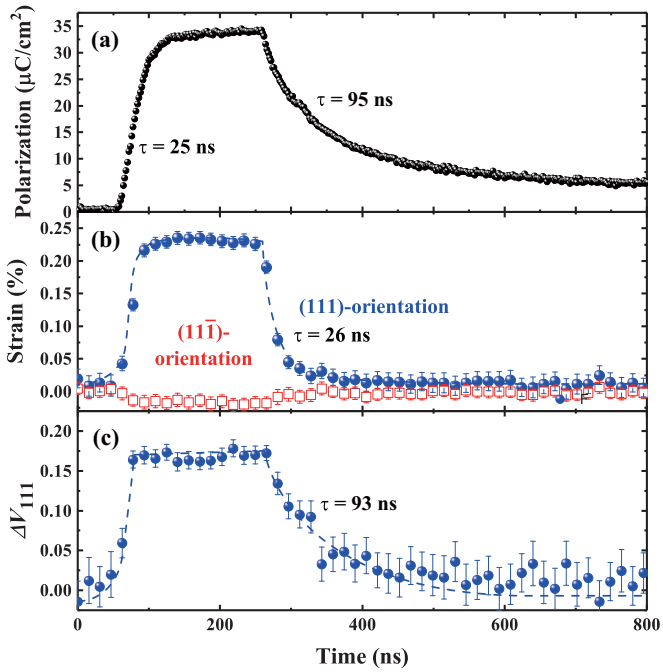

FIG. 4. (a) Polarization, (b) induced lattice strain in (111) and (11$\bar{1}$) domains, and (c) the relative change in the volume fraction of (111) orientation, V_{111}, under an electric field [ΔV_{111} (under E)] as a function of time during application of a 200-ns electric field with a magnitude of 20 V. The dashed lines are a guide for the eyes.

After removal of the electric field, the 2θ-θ at scan *IV* (300 ns) showed that the 222 peak position shifted back to a higher angle, but was not in the same position as in scan *I*. Moreover, the intensity of 222 in scan *IV* did not change significantly compared with those of scans *II* and *III*. This indicates that the relaxation of the lattice strain of the (111)-orientated domain is faster than the non-180° domain switching back from the (111) orientation to the (11$\bar{1}$) one. Finally, the subsequent θ-2θ profile at *V* (700 ns) almost recovered to the original profile at scan *I*, indicating the switching back of the non-180° domain; therefore, a fast 200-ns pulse with 1-MHz repetition can give rise to reversible domain switching.

Figure 4(a) shows the time dependence of the charge under 200-ns pulsed voltages with 20 V amplitude. The lattice strains of the (11$\bar{1}$) and (111) domains and the relative change in V_{111} under the electric field [ΔV_{111} (under E)] as a function of time are shown in Figs. 4(b) and 4(c), respectively. It must be emphasized that the amount of the switched domain [$\Delta V_{111}(\text{under } E) = 0.18$] during the repetitive electric field, is comparable to or larger than the total amount of switched domain by the poling treatment [27]. Note that the former is reversible, while the latter is irreversible. In view of the piezoelectric response under an applied electric field, the large amount of reversible non-180° domain switching would significantly contribute to the macroscopic strain in (11$\bar{1}$)/(111)-oriented PZT films even at 1.25 MHz [30]. The response of non-180° domain switching [from (11$\bar{1}$) to (111) orientation] during the rise time of the electric field is almost comparable to the response speed of the lattice strain; however, the response of back switching [from (111) to (11$\bar{1}$) orientation] after the release of the electric field indicates a delay of around a hundred nanoseconds compared to the lattice strain.

In order to discuss this delay from the electric pulse, we attempted to evaluate the relaxation time by fitting with an exponential relaxation mechanism for the rising period of the electric charge and the falling period of the electric charge, strain, and ΔV_{111}. Note that the rising period for strain and ΔV_{111} could not be fitted well due to the small number of data points. The obtained relaxation times, τ_r and τ_f, for the rise and fall periods of the electric charge were 25 and 95 ns, respectively. The large difference in relaxation time between the application and removal of the electric field means the existence of an electric charge response with different speeds for these electric inputs. A τ_r of 25 ns is a reasonable value taking into account the delay arising from the electric circuit, including the rise time for a pulse and transient phenomena due to finite impedance. The charge accumulated in the PZT capacitor of around 35 μC/cm^2 at 10 V gives the apparent capacitance of 300 pF. Taking into account the sheet resistance of $SrRuO_3$, the time constant of the serial resistance capacitance component is about 18 ns, agreeing with the observed relaxation time. Actually, this value is comparable to those observed for tetragonal PZT films with both highly (001)-texture and (100)/(001) mixed orientations. Therefore, the τ_r for the intrinsic contribution in PZT films, excluding the influence of the electric circuit, is potentially shorter. Note that the fast response of 90° domain switching without delay had been demonstrated for tetragonal PZT films [17].

The τ_r is also similar in value to the relaxation time, τ_s, of 26 ns for the strain during the removal of the electric field despite the large value of τ_f for the electric charge during this period. The similar values of τ_r and τ_s suggest that the intrinsic component of piezoresponse (and also polarization) can follow both the application and removal of the electric field. Conversely, the relaxation time τ_d for ΔV_{111} of 93 ns is significantly greater than τ_s, indicating that the relaxation requires a longer time when the electric field is being removed. This result is in contrast to the fast domain switching observed in the (100)/(001)-oriented tetragonal PZT film for both application and removal of the electric field. In addition, the value is in good agreement with τ_f, implying that the delay of electric charge is mainly due to non-180° domain switching. This slow relaxation should affect the dielectric response as well as the piezoelectric response because the domain switching would contribute to the response of the polarization. These slower dynamics agrees with the large frequency dispersion observed in rhombohedral PZT ceramics [18,19]. The slow non-180° domain relaxation is also different from that of our previous reports for the (100)/(001)-oriented tetragonal films, in which both the lattice strain and the domain switching followed the polarization speed even for measurements using the same speed pulse. The switched domain tends to recover its original domain configuration due to the substrate clamping because increasing V_{111} without strain in rhombohedral PZT, leads to area mismatch of the (111) plane and substrate surface [in tetragonal PZT, V_{001} and (001) plane]. The domain ought to switch back with a similarly fast response time, however here a marked delay was measured.

This difference between the rhombohedral and tetragonal PZT might be caused by the magnitude of the interfacial

coherency among the domain variants. For rhombohedral PZT, the areas of the bottom triangle for (111) and (11$\bar{1}$) domains in Fig. 1(d) are 0.1445 and 0.1455 nm^2, respectively, revealing an area mismatch of 0.7%. On the other hand, the areas of (001) plane and (100) plane for tetragonal PZT40/60 ($Pb(Zr_{0.4}Ti_{0.6})O_3$) are the 0.1672 and 0.1623 nm^2, respectively, and the mismatch of them is around 3%; this gets larger with increasing tetragonality. Based on the consideration that the area mismatch drives the switching back of domains, the large mismatch should drive the back switching. Therefore fast switching back without delay were observed for tetragonal PZT40/60 [17]. On the other hand, the relatively weak driving force acts upon the rhombohedral PZT because of small area mismatch, resulting in the slow domain dynamics. According to the study on the tetragonal PZT films, substrate-clamping affects the switching back of the domain [28]. The small strain also can explain a large amount of the domain switching by applying an electric field. Indeed, the change in the V_{111} of 0.15 is five times larger than a change in the (001)-domain observed in a previous study on the tetragonal PZT films [17].

It is worth mentioning that the electric charge response with respect to the pulse electric field was not recorded at the same time as the *in situ* XRD measurement. For the *in situ* XRD measurements, the pulse electric field was applied repeatedly at 1.25 MHz; on the other hand, charge measurement used only a single electric pulse. In fact, the electric charge was nonzero at the time of 800 ns as shown in Fig. 4(a); namely, it did not completely recover within 800 ns, which is equivalent to one period for the *in situ* XRD measurement. Thus, subsequent electric pulses are applied to the PZT and increase the (111)-oriented domain before the domain fully recovered to the original state at this frequency of 1.25 MHz. The observation of the full relaxation process cannot be observed in this measurement. In addition, the contribution of the domain wall motion is expected to freeze at the frequency range above 100 MHz according to the broadband dielectric responses [31]. To understand the domain dynamics and frequency dispersion completely, more broadband time-domain studies might be essential.

To discuss peak broadening while applying an electric field, the time-dependent full-width-half-maximum of the 222 reflection peak is plotted in Fig. S3(b) [32]. The peak width increased when applying an electric field. This increase in the peak width can be also confirmed by the peak shape shown in Figs. 3(c) and 3(d). The peak width immediately recovered to its initial value by removing an electric field, resulting in a similar value of the 222 peak in the pattern for scan *IV* as those in *I* and *V*. In addition, the time-dependent peak width shows a similar behavior to the time dependence of the strain, which is estimated from the peak center. Thus, the peak broadening might be caused by the inhomogeneous strain in the (111)-oriented domain while applying an electric field. One possible reason is the relatively small thickness of 200 nm in the present film. The unaltered region in the vicinity of the substrate surface cannot be ignored as a consequence of this small thickness [33].

It must also be mentioned that non-180° domain switching was ascertained to contribute to the strain at high measurement speeds in the rhombohedral PZT films even though the domain switching showed delays. These results demonstrate the importance of direct time-resolved response observation of the crystal structure change with the application of a high-speed electric pulse field to understand the frequency dependences of ferroelectric and piezoelectric films. The frequency dependences of the crystal structure change under an electric field are the next step of this study and are under investigation.

IV. CONCLUSIONS

In summary, the induced lattice strain and non-180° domain switching by a pulsed electric field with 1.25-MHz repetition were investigated by *in situ* synchrotron x-ray diffraction for epitaxially grown (11$\bar{1}$)/(111)-oriented rhombohedral $Pb(Zr_{0.65}Ti_{0.35})O_3$ (PZT) films grown on a $(111)SrRuO_3/(111)KTaO_3$ substrate. The induced lattice strain, the intrinsic effect, was ascertained to follow the high-speed pulse based on the 222 peak position shift to a lower angle within the delay due to the electric circuit. Reversible non-180° domain switching between the (11$\bar{1}$) and (111) orientations was observed during high-speed pulse measurements; however, the switching back from (111) to (11$\bar{1}$) showed a delay after the lattice strain. This delay of domain switching showed excellent agreement with the time-dependent polarization when the electric field was removed, implying that the frequency-dependent electromechanical and dielectric responses both governed the non-180° domain switching. The direct observation of this delay, which is not observed in the case of tetragonal PZT, reveals the significance of time-resolved *in situ* measurement to understand electric field responses in PZT.

ACKNOWLEDGMENTS

This work was mainly supported by the JSPS KAKENHI Grants No. 15H04121 (H.F.), 18H01474 (T.Y.), and 19K15288 (T.S.) and JST, PRESTO Grant No. JPMJPR16R9 (T.Y.). The synchrotron radiation experiments were performed at the BL13XU of SPring-8 with the approval of the Japan Synchrotron Radiation Research Institute (Proposals No. 2011A1550, No. 2012B1034, and No. 2012B1656). N.V. thanks the support of the Australaian Research Council Discovery Program.

[1] P. Muralt, J. Micromechanics Microeng. **10**, 136 (2000).
[2] D.-J. Kim, J.-P. Maria, A. I. Kingon, and S. K. Streiffer, J. Appl. Phys. **93**, 5568 (2003).
[3] V. Nagarajan, A. Roytburd, A. Stanishevsky, S. Prasertchoung, T. Zhao, L. Chen, J. Melngailis, O. Auciello, and R. Ramesh, Nat. Mater. **2**, 43 (2003).
[4] S. B. Seshadri, A. D. Prewitt, A. J. Studer, D. Damjanovic, and J. L. Jones, Appl. Phys. Lett. **102**, 042911 (2013).
[5] D. Damjanovic, S. S. N. Bharadwaja, and N. Setter, Mater. Sci. Eng. B **120**, 170 (2005).
[6] D. Damjanovic, M. Demartin, H. Shulman, M. Testorf, and N. Setter, Sens. Actuators, A **53**, 353 (1996).

[7] A. Endriss, M. Hammer, M. J. Hoffmann, A. Kolleck, and G. A. Schneider, J. Eur. Ceram. Soc. **19**, 1229 (1999).
[8] J. L. Jones, M. Hoffman, J. E. Daniels, and A. J. Studer, Appl. Phys. Lett. **89**, 092901 (2006).
[9] J. L. Jones, A. Pramanick, and J. E. Daniels, Appl. Phys. Lett. **93**, 152904 (2008).
[10] K. S. Lee, Y. K. Kim, S. Baik, J. Kim, and I. S. Jung, Appl. Phys. Lett. **79**, 2444 (2001).
[11] A. Grigoriev, D.-H. Do, D. M. Kim, C.-B. Eom, B. Adams, E. M. Dufresne, and P. G. Evans, Phys. Rev. Lett. **96**, 187601 (2006).
[12] A. Grigoriev, R. J. Sichel, J. Y. Jo, S. Choudhury, L.-Q. Chen, H. N. Lee, E. C. Landahl, B. W. Adams, E. M. Dufresne, and P. G. Evans, Phys. Rev. B **80**, 014110 (2009).
[13] T. Fujisawa, Y. Ehara, S. Yasui, T. Kamo, T. Yamada, O. Sakata, and H. Funakubo, Appl. Phys. Lett. **105**, 012905 (2014).
[14] R. L. Johnson-wilke, R. H. T. Wilke, M. Wallace, A. Rajashekhar, G. Esteves, Z. Merritt, J. L. Jones, and S. Trolier-mckinstry, IEEE Trans. Ultrason. Ferroelectr. Freq. Control **62**, 46 (2015).
[15] Y. Ehara, S. Yasui, J. Nagata, D. Kan, V. Anbusathaiah, T. Yamada, O. Sakata, H. Funakubo, and V. Nagarajan, Appl. Phys. Lett. **99**, 182906 (2011).
[16] H.-H. Huang, Q. Zhang, E. Huang, R. Maran, O. Sakata, Y. Ehara, T. Shiraishi, H. Funakubo, P. Munroe, and N. Valanoor, Adv. Mater. Interfaces **2**, 1500075 (2015).
[17] Y. Ehara, S. Yasui, T. Oikawa, T. Shiraishi, T. Shimizu, H. Tanaka, N. Kanenko, R. Maran, T. Yamada, Y. Imai, O. Sakata, N. Valanoor, and H. Funakubo, Sci. Rep. **7**, 9641 (2017).
[18] A. Pramanick, J. E. Daniels, and J. L. Jones, J. Am. Ceram. Soc. **92**, 2300 (2009).
[19] L. Fan, J. Chen, Y. Ren, and X. Xing, Inorg. Chem. **57**, 3002 (2018).
[20] D. Bolten, U. Böttger, and R. Waser, J. Eur. Ceram. Soc. **24**, 725 (2004).
[21] A. K. Kalyani, L. K. V, A. R. James, A. Fitch, and R. Ranjan, J. Phys. Condens. Matter **27**, 072201 (2015).
[22] K. Nagashima, M. Aratani, and H. Funakubo, Jpn. J. Appl. Phys. **39**, L996 (2000).
[23] O. Sakata, S. Yasui, T. Yamada, M. Yabashi, S. Kimura, H. Funakubo, R. Garrett, I. Gentle, K. Nugent, and S. Wilkins, AIP Conf. Proc. **1234**, 151 (2010).
[24] K. Saito, T. Oikawa, I. Yamaji, and T. Akai, J. Cryst. Growth **239**, 464 (2002).
[25] J. L. Jones, E. B. Slamovich, and K. J. Bowman, J. Appl. Phys. **97**, 034113 (2005).
[26] M. Mir, V. R. Mastelaro, P. P. Neves, A. C. Doriguetto, D. Garcia, M. H. Lente, J. A. Eiras, and Y. P. Mascarenhas, Acta Crystallogr. Sect. B **63**, 713 (2007).
[27] Y. Ehara, S. Yasui, T. Oikawa, T. Shiraishi, N. Oshima, T. Yamada, Y. Imai, O. Sakata, and H. Funakubo, Appl. Phys. Lett. **108**, 212901 (2016).
[28] D. V. Taylor and D. Damjanovic, J. Appl. Phys. **82**, 1973 (1997).
[29] J. E. García, R. Pérez, D. A. Ochoa, A. Albareda, M. H. Lente, and J. A. Eiras, J. Appl. Phys. **103**, 054108 (2008).
[30] M. Nakajima, A. Wada, T. Yamada, Y. Ehara, T. Kobayashi, and H. Funakubo, J. Appl. Phys. **116**, 194102 (2014).
[31] L. Jin, V. Porokhonskyy, and D. Damjanovic, Appl. Phys. Lett. **96**, 242902 (2010).
[32] See Supplemental Material at http://link.aps.org/supplemental/10.1103/PhysRevB.100.104116 for the peak fitting results of time-dependent XRD profiles.
[33] G. Catalan, A. Lubk, A. H. G. Vlooswijk, E. Snoeck, C. Magen, A. Janssens, G. Rispens, G. Rijnders, D. H. A. Blank, and B. Noheda, Nat. Mater. **10**, 963 (2011).